The Thomas Jefferson National Accelerator Facility
Theory Group Preprint Series

Additional copies are available from the authors.

The Southeastern Universities Research Association (SURA) operates the Thomas Jefferson National Accelerator Facility for the United States Department of Energy under contract DE-AC05-84ER40150.

JLAB-THY-98-12

Nuclear effects in deep inelastic scattering

O. Benhar[1†], V.R. Pandharipande[2], I. Sick[3]

[1] *Jefferson Laboratory*
Newport News, VA, 23606, USA
and
Physics Department, Old Dominion University
Norfolk, VA, 23529, USA

[2] *Physics Department, University of Illinois*
Urbana, IL, 61801, USA

[3] *Dept. für Physik und Astronomie, Universität Basel*
CH-4056 Basel, Switzerland

Abstract

We extend the approach used to treat quasi-elastic inclusive electron-nucleus scattering to the deep inelastic region. We provide a general approach to describe lepton scattering from an off-shell nucleon, and calculate the ratio of inclusive deep inelastic scattering cross sections to the deuteron for nuclear matter and helium (EMC-effect). We find that the consistent inclusion of the binding effects, in particular the ones arising from the short-range nucleon-nucleon interaction, allows to describe the data in the region of $x > 0.15$ where binding fully accounts for the deviation of the cross section ratios from one.

KEYWORDS: EMC effect, electron scattering, off-shell nucleons, nucleon-nucleon correlations, nuclear matter

[†] on leave from INFN, Sezione Sanità, I-00161 Rome, Italy

March 19, 1998

1 Introduction

The term "EMC-effect" refers to the observation that the cross sections for deep inelastic lepton-nucleus scattering (DIS) differ significantly from the sum of the nucleonic DIS cross sections. At $0.3 < x < 0.8$, where x is the Bjorken scaling variable, the nuclear cross section is reduced by up to 20%, for $0.1 < x < 0.3$ a small enhancement is observed, and for $x < 0.05$ a reduction by up to 30% is found.

A very large number of publications have presented calculations to explain these observations. For recent reviews we refer the reader to [1, 2]. Here we cannot do justice to this large body of work, and can only very summarily list the main results. For $0.3 < x < 0.8$ the main effect could be due to nucleon binding and Fermi motion; however, most calculations still have difficulties to explain the size of the "dip" at $x \sim 0.7$, and the inclusion of binding at the parton level is not without ambiguities. While early calculations occasionally got close to reproducing the "dip", later calculations which included the so called flux-factor (see below) and realistic spectral functions could not reproduce the data. For $0.1 < x < 0.3$ the contribution of excess pions in nuclei, related to the pion-exchange nature of the long-range nucleon-nucleon force, is considered to be mainly responsible. Several calculations gave contributions of the size as required by the data. Difficulties originated from the fact that this pion excess could not yet be identified in Drell-Yan processes ($p + A \rightarrow \mu^+ + \mu^-$) and appeared not to show up in the expected enhancement of the spin-longitudinal response measured in (p,n) reactions on nuclei. However, more recent analysis of the (p,n) reaction data [3] does not contradict the pion excess hypothesis and the assumptions needed to interpret the Drell-Yan data are less clear. For $x < 0.05$, the shadowing in terms of the vector dominance model largely explains the data.

In the $x > 0.3$ region many new ideas have been employed to reproduce the EMC-ratios: Q^2-rescaling, x-rescaling, multi-quark clusters, and others. With the present paper we want to study the degree to which the most conventional nuclear physics — the fact that nucleons in nuclei are bound — can account for the data. Only once this aspect is treated in the most quantitative way can one hope to learn *physics beyond* it from the comparison with the data.

In previous works, we have systematically studied inclusive electron-nucleus cross sections in the region of the quasielastic peak, at values of Bjorken $x = Q^2/2m\nu \sim 1$, with $Q^2 = |\mathbf{q}|^2 - \nu^2$, $|\mathbf{q}|$ being the three-momentum transfer, ν the electron energy loss and m the nucleon mass. These studies [4]-[7] were performed for infinite nuclear matter, using cross sections obtained by extrapolating finite-nucleus data to mass number A$= \infty$, and for light nuclei [8]. For both infinite nuclear matter and light nuclei having A≤ 4 it is possible to perform a quantitative calculation of the nucleon spectral function

$P(|\mathbf{k}|, E)$ starting from a realistic nucleon-nucleon interaction. The spectral function describes the distribution of the nucleons in momentum and energy, and contains the information on nucleons in both single-particle and correlated states. The inclusive cross sections were calculated using Plane Wave Impulse Approximation (PWIA) [9] for the description of scattering from an initially bound nucleon. The effects of the nucleon-nucleus final state interaction, important at very large x where the impulse-approximation cross section becomes very small, were treated using a generalization of Glauber theory.

We have found that for both the nuclear matter cross sections and the nuclear matter to deuteron cross section ratios most of the features of the data can be quantitatively understood.

We recently extended [10] this approach to the study of nuclear matter cross sections in the region $0.1 < x < 1$. A quantitative description of the dip in observed EMC ratios at $x \sim 0.7$ was obtained for nuclear matter when using a realistic spectral function and the generalization of PWIA to the scattering of electrons by bound nucleons. In the present paper we present a derivation of the relation between the cross sections for free and bound nucleons in the context of deep inelastic scattering, give additional details on the calculations presented in [10], and provide new results for EMC ratios for ^{4}He and ^{3}He.

2 Formalism

Inclusive electron-nucleus scattering data at moderate Q^2 ($1.5 \lesssim Q^2 \lesssim 3$ $(GeV/c)^2$) and $x \sim 1$ has been quantitatively accounted for [4]-[7]. At $x \sim 1$ the PWIA is sufficient to account for the data, while at large x Final State Interactions (FSI) are important. In this paper we extend the PWIA treatment to the deep inelastic scattering region. The basic assumption underlying this scheme is that, at large momentum transfer, scattering off a nuclear target reduces to the incoherent sum of elementary scattering processes off individual nucleons distributed according to the spectral function $P(|\mathbf{k}|, E)$, and that the FSI of the debris from the struck nucleon with the (A–1) nucleus can be neglected. The spectral function $P(|\mathbf{k}|, E)$ yields the probability of finding a nucleon of momentum k in the target with the residual system having an excitation energy E [1]. We use the four vectors $k = (E, \mathbf{k})$ to denote the energy/momentum of an off-shell nucleon in the nucleus, and $\bar{k} = (E_k, \mathbf{k})$ with $E_k = \sqrt{m^2 + \mathbf{k}^2}$ to denote the energy/momentum for the free nucleon.

[1] more precisely, E is the removal energy given by the sum of the excitation energy of the (A–1)-nucleon spectator system and the one-nucleon separation energy, plus (in a finite system) the recoil energy

The differential cross section for inclusive scattering of electrons by a free nucleon N (= n or p) of four-momentum $\tilde{k}$ can be expressed as:

$$\frac{d^2\sigma}{d\Omega d\nu} = \frac{\alpha^2}{q^4}\frac{E_i}{E_f}\frac{m}{E_k}\, L^{\mu\nu}(k_i,k_f)W_{\mu\nu}(\tilde{k},q) \qquad (1)$$

where α is the fine structure constant, $k_i \equiv (E_i,\mathbf{k}_i)$ and $k_f \equiv (E_f,\mathbf{k}_f)$ are the initial and scattered electron four-momenta, respectively, the four-momentum transfer is $q = k_i - k_f \equiv (\nu,\mathbf{q})$ and the leptonic tensor $L^{\mu\nu}$ is fully specified by the measured kinematical variables (see e.g. ref.[11]).

The nucleon tensor is given by:

$$W_{\mu\nu}(\tilde{k},q) = \sum_X \int d^3p_X \langle N,\mathbf{k}|J_\mu|X,\mathbf{p}_X\rangle\langle X,\mathbf{p}_X|J_\nu|N,\mathbf{k}\rangle \delta^{(3)}(\mathbf{k}+\mathbf{q}-\mathbf{p}_X)\delta(E_k+\nu-E_X)\,, \qquad (2)$$

where $|N,\mathbf{k}\rangle$ and $|X,\mathbf{p}_X\rangle$ are time independent representations of the initial nucleon and final hadronic states, J_μ are Schrödinger current operators, and E_X is the energy of the final state $|X,\mathbf{p}_X\rangle$. Averaging over the spin states of the initial nucleons is implicit. The tensor $W_{\mu\nu}$ is defined with covariantly normalized nucleon states $|N,\mathbf{k}\rangle$, and the factor m/E_k in the cross section restores the unit norm.

Our understanding of nucleon structure has not yet developed to the point where $W_{\mu\nu}(\tilde{k},q)$ can be calculated; it is obtained by fitting experimental data.

We can similarly express the inclusive electron-nucleus cross section using a nuclear tensor $W^A_{\mu\nu}(q)$ in the lab frame:

$$W^A_{\mu\nu}(q) = \sum_I \int d^3\mathbf{p}_I \langle A|J_\mu|I,\mathbf{p}_I\rangle\langle I,\mathbf{p}_I|J_\nu|A\rangle \delta^{(3)}(\mathbf{q}-\mathbf{p}_I)\delta(E_A+\nu-E_I)\,, \qquad (3)$$

where $|A\rangle$ is the nuclear ground state with zero momentum and energy E_A, and $|I,\mathbf{p}_I\rangle$ are all the possible final states with energies E_I.

The assumptions of PWIA, illustrated in fig.1, imply that the final states $|I,\mathbf{p}_I\rangle$ which contribute to $W^A_{\mu\nu}$ have (A–1) residual nucleons with total momentum $\mathbf{p}_R$ in a state denoted by $|R,\mathbf{p}_R\rangle$ and the struck nucleon in the final state $|X,\mathbf{p}_X\rangle$. Hence we can truncate the sum over I to:

$$\sum_I \int d^3p_I |I,\mathbf{p}_I\rangle\langle I,\mathbf{p}_I| \rightarrow \sum_{R,X}\int d^3p_R\, d^3p_X |X,\mathbf{p}_X;R,\mathbf{p}_R\rangle\, \langle x,\mathbf{p}_X;R,\mathbf{p}_R|. \qquad (4)$$

PWIA also implies that the final state interactions between the debris of the struck nucleon and the residual nucleus can be neglected. In this case the matrix element of the current operator factorizes:

$$\langle A|J_\mu|X,\mathbf{p}_X;R,\mathbf{p}_R\rangle = \langle A|N,-\mathbf{p}_R;R,\mathbf{p}_R\rangle\sqrt{\frac{m}{E_{P_R}}}\langle N,-\mathbf{p}_R|J_\mu|X,\mathbf{p}_X\rangle. \qquad (5)$$

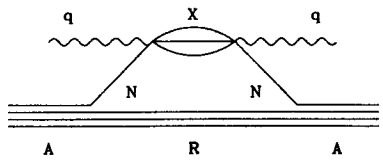

Figure 1: Inclusive electron-nucleus scattering in PWIA.

Its first factor gives the amplitude to find in the ground state of the nucleus the residual system in state $|R,\mathbf{p}_R\rangle$ and a nucleon in state $|N,-\mathbf{p}_R\rangle$ with unit norm. The factor $\sqrt{m/E_{P_R}}$ takes into account the implicit covariant norm of $\langle N,-\mathbf{p}_R|$ in the matrix element of J_μ. The spectral function is defined as:

$$P(\mathbf{k},E) = \sum_R |\langle A|N,\mathbf{k};R,-\mathbf{k}\rangle|^2\delta(E_A-E_R-E). \qquad (6)$$

Using equations (4) to (6) in eq. (3) gives the $W^A_{\mu\nu}(q)$ in PWIA:

$$\begin{aligned} W^A_{\mu\nu}(q) &= \sum_R \int d^3p_R |\langle A|N,-\mathbf{p}_R;R,\mathbf{p}_R\rangle|^2 \left(\frac{m}{E_{P_R}}\right) \\ &\quad \sum_X \int d^3p_X \langle N,-\mathbf{p}_R|J_\mu|X,\mathbf{p}_X\rangle\langle X,\mathbf{p}_X|J_\nu|N,-\mathbf{p}_R\rangle \\ &\quad \delta^{(3)}(\mathbf{q}-\mathbf{p}_X-\mathbf{p}_R)\,\delta(E_A+\nu-E_X-E_R) \\ &= \int d^3k\, dE\; P(\mathbf{k},E)\left(\frac{m}{E_k}\right)\sum_X \int d^3p_X \langle N,\mathbf{k}|J_\mu|X,\mathbf{p}_X\rangle \\ &\quad \langle X,\mathbf{p}_X|J_\nu|N,\mathbf{k}\rangle\delta^{(3)}(\mathbf{q}+\mathbf{k}-\mathbf{p}_X)\,\delta(E+\nu-E_X) \end{aligned} \qquad (7)$$

In order to relate the above $W^A_{\mu\nu}$ to the free nucleon tensor given by eq.(2) we define:

$$\tilde{\nu} = E - E_k + \nu; \qquad \tilde{q} = (\tilde{\nu},\mathbf{q}). \qquad (8)$$

Note that $\tilde{\nu}$ is the energy transferred to the struck nucleon, the energy $\nu-\tilde{\nu} = E_k - E$ goes into the residual system. The energy conserving δ-function in eq.(7) then becomes $\delta(E_k+\tilde{\nu}-E_X)$, and the sum over X gives:

$$W^A_{\mu\nu}(q) = \int d^3k\, dE\; P(\mathbf{k},E)\left(\frac{m}{E_k}\right) W_{\mu\nu}(\tilde{k},\tilde{q}). \qquad (9)$$

Equation (9) has also been written in the form:

$$W^A_{\mu\nu}(q) = \int d^4k\ P(k) \left(\frac{m}{E_k}\right) \widetilde{W}_{\mu\nu}(k,q), \qquad (10)$$

where k is a 4-vector with $k_0 = E$ and $\widetilde{W}_{\mu\nu}$ is the tensor for bound (off-shell) nucleons for which $k^2 \neq m^2$. This is our basic equation, used in refs.[4, 5, 7, 10] to calculate inclusive cross sections within PWIA.

In PWIA we have proved that:

$$\widetilde{W}_{\mu\nu}(k,q) = W_{\mu\nu}(\tilde{k},\tilde{q}) = -W_1^N\left(\tilde{Q}^2, \tilde{q}\cdot\tilde{k}\right)\left(g_{\mu\nu} + \frac{\tilde{q}_\mu \tilde{q}_\nu}{\tilde{q}^2}\right)$$
$$+\frac{W_2^N\left(\tilde{Q}^2, \tilde{q}\cdot\tilde{k}\right)}{m^2}\left(\tilde{k}_\mu - \frac{\tilde{q}\cdot\tilde{k}}{\tilde{q}^2}\tilde{q}_\mu\right)\left(\tilde{k}_\nu - \frac{\tilde{q}\cdot\tilde{k}}{\tilde{q}^2}\tilde{q}_\nu\right), \qquad (11)$$

W_1^N and W_2^N being the nucleon structure functions that can be extracted from the proton and deuteron data. The appearance of $\tilde{q}, \tilde{k}$ (rather than q, k) in the factors multiplying W^N in eq.(11) is a direct consequence of PWIA and Lorentz invariance for the case of scattering from an off-shell nucleon. The total four momentum of the hadronic final state $|X, p_X\rangle$ is $\tilde{k} + \tilde{q}$ where $\tilde{k}$ is the on-shell four momentum of the struck nucleon. These factors are of great importance for the understanding of inclusive electron-nucleus scattering.

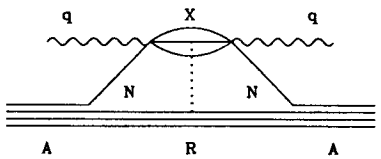

Figure 2: FSI of the knocked out system with the residual nucleus.

The above relations are not exact due to the use of PWIA. The two leading corrections to PWIA, shown in figures 2 and 3, are due to FSI and coherent contributions. At high energies and $x > 1$ the effect of FSI on inclusive scattering cross sections has been estimated using the Correlated Glauber Approximation (CGA) [4]. Since the FSI of high energy hadrons

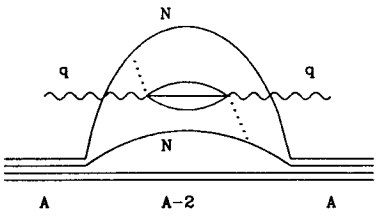

Figure 3: Example of two-nucleon coherent contribution.

in nuclear matter is mainly absorptive, its effect can be accounted for by a folding expression:

$$\frac{d^2\sigma_{FSI}(\nu,q)}{d\Omega d\nu} = \int d\nu' \frac{d^2\sigma(\nu',q)}{d\Omega d\nu} F(\nu-\nu'), \qquad (12)$$

where the folding function $F(\nu-\nu')$ is related to the decay rate of the state $|X, p_X\rangle$ in matter. This folding has significant consequences at large x where the cross section varies rapidly with energy transfer ν. However, in the x-region of interest here, the cross section varies slowly with ν and the effect of FSI is expected to be negligible.

At large values of momentum transfer q most of the coherent processes with participation of more than one nucleon are expected to be negligible as well. However, the process shown in fig.3 can contribute. It involves deep inelastic scattering with a slow nucleon in the final state. Pion current contributions, called "excess pion contributions" in the deep inelastic scattering regime, are examples of such coherent contributions. They are expected to become important at small x due to the small mass of the pions, and they are responsible for a good part of the meson exchange contributions present in observables such as the form factors of light nuclei at large momentum transfer [12]. We will return to these pion contributions below.

Contraction of $\widetilde{W}_{\mu\nu}$, constructed according to the above procedure, with the leptonic tensor $L^{\mu\nu}$ leads to the standard expression for the inclusive cross section:

$$\frac{d^2\sigma}{d\Omega d\nu} = \sigma_M \left[2W_1^A(Q^2,\nu) tan^2\frac{\theta}{2} + W_2^A(Q^2,\nu)\right], \qquad (13)$$

where σ_M is the Mott cross section

$$\sigma_M = 4\alpha^2 \left(\frac{E_f}{q^2}\right)^2 cos^2\frac{\theta}{2}, \qquad (14)$$

θ being the electron scattering angle.

The nuclear structure functions are found to be:

$$W_1^A(Q^2,\nu) = \int d^4k\, P(k) \left(\frac{m}{E_k}\right) \left[W_1^N\left(\tilde{Q}^2,\tilde{q}\cdot\tilde{k}\right) + \frac{1}{2m^2} W_2^N\left(\tilde{Q}^2,\tilde{q}\cdot\tilde{k}\right) \frac{|\mathbf{k}\times\mathbf{q}|^2}{\mathbf{q}^2}\right] \quad (15)$$

and

$$W_2^A(Q^2,\nu) = \int d^4k\, P(k) \left(\frac{m}{E_k}\right) \left\{W_1^N(\tilde{Q}^2,\tilde{q}\cdot\tilde{k}) \frac{(\nu-\tilde{\nu})^2}{\tilde{q}^2} + \frac{W_2^N(\tilde{Q}^2,\tilde{q}\cdot\tilde{k})}{m^2} \left[\left(\frac{\nu-\tilde{\nu}}{\tilde{q}^2}(\tilde{k}\cdot\tilde{q}) + \tilde{k}_0 - \frac{\nu}{|\mathbf{q}|}k_z\right)^2 - \frac{1}{2}\frac{q^2}{|\mathbf{q}|^2}\frac{|\mathbf{k}\times\mathbf{q}|^2}{|\mathbf{q}|^2}\right]\right\} \quad (16)$$

Notice that the standard Atwood-West [13] result can be recovered from the above $W_{1,2}^A$ by setting $\tilde{\nu} = \nu$ and $k = \tilde{k}$.

The nuclear tensor, obtained inserting $\widetilde{W}_{\mu\nu}$ of eq.(11) into eq.(10), does not fulfill the gauge invariance requirement

$$q^\mu W_{\mu\nu}^A(q) = 0\,, \quad (17)$$

implying in turn

$$q^\mu \widetilde{W}_{\mu\nu}(k,q) = 0\,. \quad (18)$$

This failure is due to the approximations of PWIA is illustrated in figs.2 and 3. In order to gauge its importance we adopt a procedure originally proposed by deForest when studying electron-nucleus scattering in the quasielastic regime [9, 14]. The basic idea is to use eq.(11) to evaluate the time and transverse components of $\widetilde{W}_{\mu\nu}$ only (i.e. using $\mathbf{q} = |\mathbf{q}|\hat{z}$ for $\mu,\nu = 0,1$ and 2), whereas the longitudinal components are obtained from the continuity equation (18), yielding

$$\widetilde{W}_{3\nu}(k,q) = \left(\frac{\nu}{|\mathbf{q}|}\right) W_{0\nu}(\tilde{k},\tilde{q}) \quad (19)$$

for $\nu \neq 3$ and

$$\widetilde{W}_{33}(k,q) = \left(\frac{\nu}{|\mathbf{q}|}\right)^2 W_{00}(\tilde{k},\tilde{q})\,. \quad (20)$$

The nuclear structure functions appearing in eq.(13) then are found to be:

$$W_1^A(Q^2,\nu) = \int d^4k\, P(k) \left(\frac{m}{E_k}\right) \left[W_1^N\left(\tilde{Q}^2,\tilde{q}\cdot\tilde{k}\right) + \frac{1}{2}\frac{W_2^N\left(\tilde{Q}^2,\tilde{q}\cdot\tilde{k}\right)}{m^2}\frac{|\mathbf{k}\times\mathbf{q}|^2}{|\mathbf{q}|^2}\right] \quad (21)$$

and

$$W_2^A(Q^2,\nu) = \int d^4k P(k) \left(\frac{m}{E_k}\right) \left\{W_1^N\left(\tilde{Q}^2,\tilde{q}\cdot\tilde{k}\right)\frac{q^2}{|\mathbf{q}|^2}\left(\frac{q^2}{\tilde{q}^2}-1\right) + \frac{W_2^N\left(\tilde{Q}^2,\tilde{q}\cdot\tilde{k}\right)}{m^2}\left[\frac{q^4}{|\mathbf{q}|^4}\left(\tilde{k}_0 - \tilde{\nu}\frac{\tilde{q}\cdot\tilde{k}}{\tilde{q}^2}\right)^2 - \frac{1}{2}\frac{q^2}{|\mathbf{q}|^2}\frac{|\mathbf{k}\times\mathbf{q}|^2}{|\mathbf{q}|^2}\right]\right\} \quad (22)$$

It can be easily verified that the expression of the nuclear quasielastic cross section of ref.[14] can be recovered by inserting in eqs.(21) and (22) the appropriate nucleon structure functions:

$$W_1^N(Q^2,\nu) = \frac{Q^2}{2m} G_M^2(Q^2)\delta(W^2-m^2) \quad (23)$$

and

$$W_2^N(Q^2,\nu) = \frac{2m}{\left(1+\frac{Q^2}{4m^2}\right)}\left[G_E^2(Q^2) + \frac{Q^2}{4m^2}G_M^2(Q^2)\right]\delta(W^2-m^2)\,, \quad (24)$$

where G_E and G_M are the electric and magnetic nucleon form factors.

This procedure to restore gauge invariance is somewhat *ad hoc*. In the case of DIS, there are no strong theoretical arguments supporting the deForest prescription. In principle, instead of defining the longitudinal components of the nucleon tensor as in eqs.(19) and (20), one could have as well used the continuity equation to obtain the charge components of $\widetilde{W}_{\mu\nu}$ from the longitudinal ones. However, about 80% of deep inelastic scattering is transverse, and hence unaffected by the deForest prescription. Our numerical results, discussed below, show that the extra terms appearing in eqs.(21,22) on account of the use of the deForest prescription contribute less than 4% to the nuclear matter to deuteron structure function ratio in the range $0.4 < x < 0.8$, whereas the replacement of q and k with $\tilde{q}$ and $\tilde{k}$ produce the major effect of $\sim 20\%$ in magnitude.

The above equations are valid to describe electron-nucleus scattering at all energies where PWIA is valid. In the case of the very high energies of interest in the deep-inelastic region, one can use the Bjorken limit: $Q^2,\nu \to \infty$ with $x = Q^2/2m\nu$ finite, implying $\nu/|\mathbf{q}| \to 1$ and $q^2/|\mathbf{q}|^2 \to 0$. In this limit equation (22) simplifies considerably, the terms containing W_1^N and $\mathbf{k}\times\mathbf{q}$ do not contribute,

$$\frac{q^4}{|\mathbf{q}|^4}\left(\tilde{k}_0 - \tilde{\nu}\frac{\tilde{q}\cdot\tilde{k}}{\tilde{q}^2}\right)^2 \to \frac{Q^4}{\tilde{Q}^4}\frac{\left(\tilde{k}\cdot\tilde{q}\right)^2}{\nu^2}, \quad (25)$$

and it becomes:

$$W_2^A(Q^2,\nu) = \int d^4k\, P(k) \left(\frac{m}{E_k}\right) W_2^N\left(\tilde{Q}^2,\tilde{q}\cdot\tilde{k}\right)\frac{Q^4}{\tilde{Q}^4}\frac{\left(\tilde{k}\cdot\tilde{q}\right)^2}{m^2\nu^2}. \quad (26)$$

Further using the conventional definitions:

$$F_2^A = \nu W_2^A, \tag{27}$$

$$F_2^N = \frac{\tilde{k}\cdot\tilde{q}}{m} W_2^N, \tag{28}$$

$$\tilde{x} = \frac{\tilde{Q}^2}{2\tilde{k}\cdot\tilde{q}}, \tag{29}$$

and noting that

$$\frac{\tilde{Q}^2}{Q^2} \rightarrow 1 + \frac{\delta\nu}{mx},$$

where $\delta\nu = \nu - \tilde{\nu}$, we obtain, in the Bjorken limit:

$$F_2^A\left(Q^2, x\right) = \int d^4k\ P(k)\ \left(\frac{m}{\tilde{k}_0}\right) F_2^N\left(\tilde{Q}^2, \tilde{x}\right) \frac{x}{\tilde{x}}\ \frac{1}{(1+\delta\nu/mx)}. \tag{30}$$

Eq.(30) emphasizes that the binding effects do not go away even when q and ν become arbitrarily large. Eq.(30) shows that there is a Q^2-independent factor $(1+\delta\nu/mx)$ that occurs in the expression for F, and that there is a rescaling of F_2^N.

Over the past decade, a number of theoretical studies of nuclear effects in deep inelastic scattering (for recent reviews see e.g. refs.[1, 2]) have been carried out within the so called convolution model, occasionally also using a realistic nuclear spectral function. It is therefore worthwhile to make a connection, and point out the differences. This model assumes that the nucleon tensor defined in eq.(11) can be approximated by replacing $\tilde{q}$ and $\tilde{k}$ by q and k. This gives:

$$F_2^A(Q^2, x) = \int d^4k P(k)\ \left(\frac{m}{k_0}\right) F_2^N(Q^2, x')\left(\frac{x}{x'}\right)\ , \tag{31}$$

where $x' = Q^2/2(q\cdot k)$. Equation (31) is totally equivalent to the standard convolution approach expression of F_2^A:

$$F_2^A(Q^2, x) = \int_{z\geq x} dz\ f_A(z)\ F_2^N\left(Q^2, \frac{x}{z}\right)\ , \tag{32}$$

where

$$f_A(z) = z\int d^4k P(k)\ \left(\frac{m}{k_0}\right)\delta\left(z - \frac{(q\cdot k)}{m\nu}\right)\ . \tag{33}$$

It has to be noticed that $f_A(z)$ as given by eq.(33) includes the factor z in front of the integral, a factor generally referred to as the "flux factor" (the

lack of which in some of the earlier calculations caused them to better agree with the data), and fulfills the normalization requirement

$$\int dz\ f_A(z) = 1 \tag{34}$$

by construction, since the spectral function only depends upon the magnitude of k and its normalization is

$$\int d^3k dE\ P(|\mathbf{k}|, E) = 1\ . \tag{35}$$

The main difference between the convolution model and the approach discussed in this work arises from the different treatment of nuclear binding

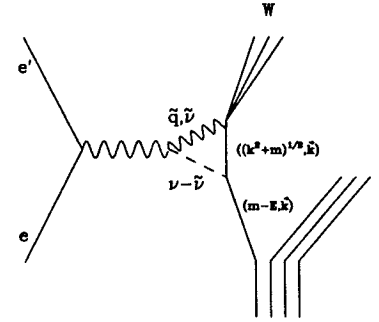

Figure 4: Diagram depicting the conceptual split of the off-shell scattering process into a transfer of energy required to put the nucleon on-shell, and the subsequent on-shell DIS process calculated using the known nucleon structure functions.

energy represented by $\delta\nu$. Upon setting $\delta\nu = 0$ and $\tilde{k}_0, \tilde{Q}^2$ and $\tilde{x}$ respectively to k_0, Q^2 and x', our eq.(30) becomes identical to eq.(31). In the convolution model, the $\delta\nu$ is associated with the initial energy of the struck particle and eq.(11) is used with four-vectors q and k to obtain the tensor for an off-shell nucleon with $k^2 \neq m^2$. This is an *ad hoc* and incorrect procedure. As discussed earlier, within PWIA the tensor for the bound nucleon must be calculated using the $\tilde{k}$ and $\tilde{q}$ four vectors.

The nucleon structure functions in eq.(30) are evaluated at $\tilde{Q}^2$ which is larger than Q^2 by a factor $1+\delta\nu/mx$. The average value of $1+\delta\nu/mx$ obtained from realistic spectral functions of nuclear matter ranges from $\sim$ 1.1 to 1.5 in the $x = 1$ to 0.2 range. In some Q^2 rescaling models [15, 16, 17]

the convolution formula (31) is used with a scaled sQ^2 in place of the Q^2 in the argument of W_2^N. In these models the observed magnitude of the dip at $x \sim 0.7$ is not well reproduced when our scaling factor $s = 1.25$ for this region is used [18]. Much larger scaling factors ($s \sim 2$) are needed to explain the observed effect with only rescaling without convolution. Our eq.(30) has an additional $1/(1 + \delta\nu/mx)$ factor, absent in the rescaling models, which reduces the F_A^2 of nuclear matter significantly. This factor comes from using $\tilde{k}$ and $\tilde{q}$ in the factors multiplying W^N in eq.(11).

The F_2^N in eq.(30) are also evaluated at $\tilde{x}$ instead of the x' used in the convolution model. We note that

$$\frac{\tilde{x}}{x'} = \frac{\tilde{Q}^2}{Q^2}\,\frac{k\cdot q}{\tilde{k}\cdot\tilde{q}} \sim (1+\frac{\delta\nu}{mx})(1-\frac{\nu\delta\nu}{k\cdot q}). \qquad (36)$$

We find the estimate $\tilde{x}/x' = 1 + \delta\nu(1-x)/mx$, indicating an x-dependent rescaling of x'.

3 Spectral functions

In order to address the nuclear properties relevant to DIS, we employ the spectral function $P(|\mathbf{k}|, E)$, which gives the probability to find in the nucleus a nucleon of given momentum k and energy E. This spectral function can be calculated starting from the nucleon-nucleon interaction for very light nuclei, A$\leq$ 4, and infinite nuclear matter [19].

The nuclear matter calculation has been performed using Correlated Basis Function (CBF) theory and the Urbana v_{14} nucleon-nucleon interaction, supplemented by the three-nucleon interaction (TNI) which accounts for the neglect of non-nucleonic degrees of freedom and is needed to obtain the correct binding energies. $P(|\mathbf{k}|, E)$ contains the information on both the nuclear mean field (at low $|\mathbf{k}|, E$), and the short-range nucleon-nucleon correlations (at high $|\mathbf{k}|, E$). The latter must be expected to contribute to processes such as (e, e') at large $|\mathbf{q}|$, which sample the nucleus with a spatial resolution of order $1/|\mathbf{q}|$. A significant part of the influence of the nuclear medium therefore must be expected to depend on the *short-range* properties of the wave function.

The calculated spectral function shows that only about 70% of the nucleons are in the states of low $|\mathbf{k}|$ and low E that are described in a mean-field theory. Some 30% of the nucleons are in a correlated state with another nucleon, a correlation that mainly results from the one-pion exchange tensor force and the short-range repulsion of the nucleon-nucleon interaction. These correlations involve strength that is located both below and above the Fermi momentum k_F, and they give important contributions to the average removal energy (61.9 MeV) and average kinetic energy (36.3 MeV). Although

the strength *above* k_F amounts to only 14%, these nucleons give a contribution of 23.3 MeV (17.0 MeV) to the average removal (kinetic) energy. Note that the average value of $\delta\nu$ equals the sum of the average values of removal and kinetic energies. By Koltun's sum rule [20] $< \delta\nu >$ thus equals $-2 < v_{ij} >$, where $< v_{ij} >$ is the expectation value of the nucleon-nucleon interaction potential in the nuclear ground state, neglecting the small TNI contributions.

The spectral function of ^{4}He is obtained from many-body calculations using the Argonne v_{14} two-nucleon interaction and Urbana VII three-nucleon interaction. It has been used in previous studies of inclusive scattering of GeV electrons by ^{4}He in the $x \sim 1$ region, and its calculation is described in ref.[8]. The average values of the kinetic energy per nucleon and $< \delta\nu >$ in ^{4}He are 25 and 61 MeV, respectively.

4 Data

Data on inclusive scattering from infinite nuclear matter can be obtained from finite-nucleus data by extrapolating the cross sections (or ratios) to mass number A= ∞. The nuclear property of interest in the case of the EMC effect is a *local* one, as electron scattering at large $|\mathbf{q}|$ samples the nucleus with a spatial resolution of order $1/|\mathbf{q}|$, at least as long as x is not too small. For such observables one can employ the Local Density Approximation (LDA) which starts from the assumption that the effect of the nuclear medium depends only on the density near the interaction point.

For nuclei with A$>$ 4 the nuclear density distribution $\rho(r)$ is experimentally found to be roughly constant in the nuclear interior. In the surface region the shape of $\rho(r-R)$, where $R = r_0 \cdot A^{1/3}$ represents the half-density radius, is essentially a universal function of $r - R$, independent of A. The cross section then receives a contribution from the constant-density region with volume proportional to A, and a contribution from the surface region proportional to R^2, i.e. $A^{2/3}$. It follows immediately that the cross section per nucleon σ/A is a linear function of $A^{-1/3}$. The slope of this line contains information about the density dependence of the cross section (ratio), whereas the value of the intercept with the $A^{-1/3}$=0 axis yields the nuclear matter cross section.

In this context we want to point out that the often-used parameterization of the data in terms of an *exponential* A-dependence does not lead to a sensible result in the limit A=∞, and contradicts the fact that the lepton probe explores the nucleus with a spatial resolution of order $1/|\mathbf{q}|$ — which at large momentum transfer is small — in which case the nucleons far away from the one hit cannot have an influence.

The $A^{-1/3}$ extrapolation has first been performed for data in the quasi-

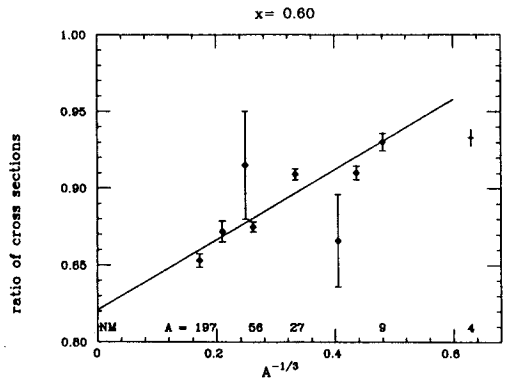

Figure 5: Ratio of nuclear and deuteron response, extrapolated as a function of $A^{-1/3}$ to nuclear matter for x=0.6. Only the statistical errors of the data are shown. Some of the values of A of the data are indicated at the bottom. The point for ^{4}He is not used, as the density $\rho(r-R)$ in the surface region for helium differs strongly from the one for nuclei with A>4.

elastic region ($x \simeq 1$) where it turned out to be very successful. In ref.[21] several tests performed on this much more extensive set of data have been described.

For the present work we have extended the study of [22] for $x < 1$ by analyzing todays *world data* on nucleus-to-deuteron cross section ratios [23] -[35]. For A > 4 some 350 data points are available for the region $x >$ 0.05 of interest here. As these ratios do not show any significant Q^2 dependence, the data for all Q^2 and A>4 can be combined and extrapolated to $A^{-1/3}$=0 for any bin in x. The fits confirm that LDA is a valid approximation; the world data can be represented within the experimental uncertainties with this linear $A^{-1/3}$ dependence. An example for such an extrapolation is shown in fig.5. The resulting nuclear matter-to-deuteron ratios, together with the corresponding values of the slope, thus allow for a very concise representation of the *world* data for all nuclei. The uncertainties in the nuclear matter-to-deuteron ratios are significantly smaller than for the ratios for individual nuclei, and a single curve contains the full experimental information on nucleus-to-deuteron cross section ratios today available. The resulting data for nuclear matter will be compared to theoretical predictions in figs.

8, 10 and 11. The slopes of the $A^{-1/3}$ fits, which contain some additional information on the density dependence of the EMC-effect, will be exploited in a different context [36].

The nuclear-matter to deuteron ratios represent all data for $A > 4$. As discussed above, the data for very light nuclei are not included in the $A^{-1/3}$ extrapolation as the surface thickness of their density strongly differs from the one for the heavier nuclei. In order to also include the very light nuclei, we will also show results for helium. While there are no experimental EMC-ratios for ^{3}He, data are available for ^{4}He. Both refs.[30, 37] have measured cross section ratios between helium and the deuteron. These will be used when comparing to our calculated results below.

5 Results

The deuteron and nuclear matter PWIA inclusive cross section in the deep inelastic regime have been calculated from eqs.(13)–(16), using as inputs theoretical spectral functions, and nucleon structure functions extracted from the proton and deuteron data.

Fig.6 shows the deuteron structure function $F_2^d(Q^2,x) = \nu W_2^d(Q^2,x)$ as a

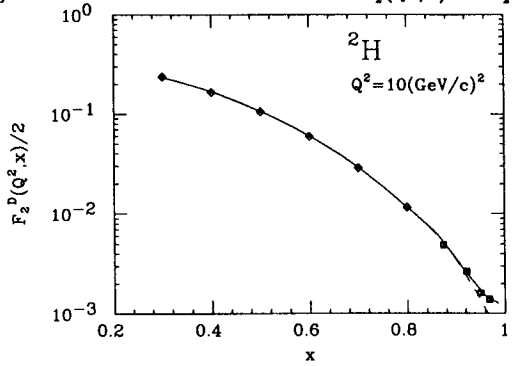

Figure 6: Deuteron structure function at $Q^2 \sim 10(\mathrm{GeV/c})^2$ compared to the data. The solid curve includes the quasielastic contribution.

function of x resulting from our approach, together with the data of refs.[38, 30] at $Q^2 \sim 10\ (GeV/c)^2$. The calculation has been carried out using the deuteron spectral function:

$$P_d(\mathbf{k},E) = |\Psi_d(\mathbf{k})|^2\ \delta(m + E_d - |\mathbf{k}|^2/2m - E)\ , \qquad (37)$$

where $E_d = -2.23\ MeV$ is the deuteron binding energy and the momentum-space wave function $\Psi_d(\mathbf{k})$ has been obtained solving the Schrödinger equation with the Urbana $v14$ interaction [39]. The nucleon structure functions have been taken from ref.[40], where the proton and neutron W_2^N have been parameterized including both the resonance and the deep inelastic contributions. The corresponding W_1^N have then been obtained from

$$W_1^N(Q^2,\nu) = W_2^N(Q^2,\nu)\frac{\left(1+\frac{\nu^2}{Q^2}\right)}{1+R_{LT}(Q^2,x)}\ , \tag{38}$$

where $R_{LT}(Q^2,x) = \sigma_L/\sigma_T$ is the measured ratio of the longitudinal (σ_L) and transverse (σ_T) virtual photon absorption cross sections.

The calculated inelastic cross section, represented by the dashed line, turns out to be in perfect agreement with the experiment over the range $0.3 < x < 0.8$, while discrepancies appear at larger x, where the theoretical curve increasingly lies below the data. This is due to the presence of nonnegligible contributions from quasielastic scattering at large x. The solid line, obtained by adding the quasielastic contributions evaluated from eq.(22) using the spectral function of eq.(37) and the nucleon structure functions of eqs.(23)-(24), reproduces the data up to the largest value of x ($x = .968$), where quasielastic scattering accounts for $\sim 35\%$ of the measured cross section.

It has to be pointed out that even for A= 2 nuclear effects are not entirely negligible. Scattering off the deuteron does not reduce to the sum of scattering off two free nucleons at rest, as shown by the ratio

$$R_d(Q^2,x) = \frac{d^2\sigma_d}{(d^2\sigma_p + d^2\sigma_n)}\ , \tag{39}$$

displayed in fig.7. The motion of the struck particles produces large (and well-known) effects at $x > 0.8$. But even for $x < 0.8$ significant deviations of $R_d(Q^2,x)$ from unity are found. On the other hand, the effect of our treatment of the nucleon tensor turns out to be small. Replacing $\bar{q}$ with q in eqs.(21) and (22) leads to changes in the cross section of less than 1% over the whole range $0.3 < x < 0.9$.

The deuteron, helium and the nuclear matter cross sections are calculated using eqs.(13)-(16) and include the quasi-elastic contribution. Fig.8 shows the calculated nuclear matter to deuteron cross section ratios, compared to the data. To provide an estimate for the theoretical uncertainty related to the non-conservation of the electromagnetic current, we also show in fig.8 the results using the deForest prescription (eqs.21,22, obtained by deriving $\widetilde{W}_{3\nu}$ from current conservation). This result is shown as a dashed line.

Fig. 8 also illustrates the relevance of the realistic treatment of the momentum and removal energy distribution of the struck nucleon. While the dashed line represents the result obtained with the full spectral function of

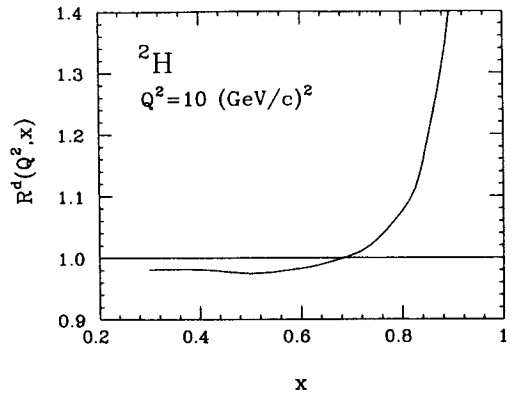

Figure 7: Ratio of deuteron DIS cross section to sum of proton and neutron cross sections.

nuclear matter [19] and the nucleon structure functions of ref.[40], the dashed-dot line has been obtained using the Fermi gas model spectral function:

$$P_{FG}(|\mathbf{k}|,E) = \frac{3}{4\pi k_F^3}\theta(k_F - |\mathbf{k}|)\delta(E - m - \epsilon_k)\ , \tag{40}$$

where

$$\epsilon_k = \frac{k^2}{2m} - U_0\ , \tag{41}$$

and the constant U_0 (=53MeV) is fixed requiring $\epsilon_{k_F} = -16\ MeV$. Comparison between the dashed and dashed-dot curves clearly shows that using the oversimplified spectral function of eq.(40), which corresponds to an assembly of uncorrelated nucleons, underestimates the binding effect on the calculated cross section ratio, thus resulting in a theoretical prediction that consistently lies above the data over the range $0.3 < x < 0.8$. For the Fermi gas spectral function $< \delta\nu > = U_0 = 53$ MeV. The rather small dip obtained with this spectral function, as compared to that with the realistic spectral function, for which $< \delta\nu > = 98$ MeV, suggests that the dip does not simply scale with $< \delta\nu >$.

The empirical binding energy, $E_0 = -16$MeV/A, and density, $\rho = 0.16$ fm^{-3} corresponding to the Fermi momentum $k_F = 1.33$ fm^{-1}, of nuclear matter provide a lower bound for $< \delta\nu >$. Using Koltun's sum rule we obtain $< \delta\nu >= -2 < v_{ij} >= 2 < T > -2E_0$ where $< T >$is the kinetic energy per nucleon. Since $< T >> 3k_F^3/10m$ the Fermi gas kinetic energy $\delta\nu > 6k_F^2/10m - 2E_0 = 76$MeV. In this context the above Fermi gas model

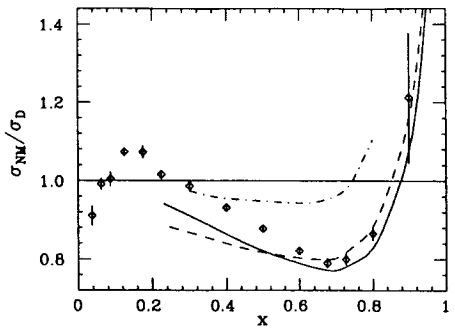

Figure 8: Results for the nuclear matter to deuterium cross section ratios, compared to the experimental data. The solid line gives the full result, the dashed line gives the result obtained using the deForest prescription. The dashed-dot line gives the ratio when replacing in addition the spectral function by the Fermi-gas spectral function.

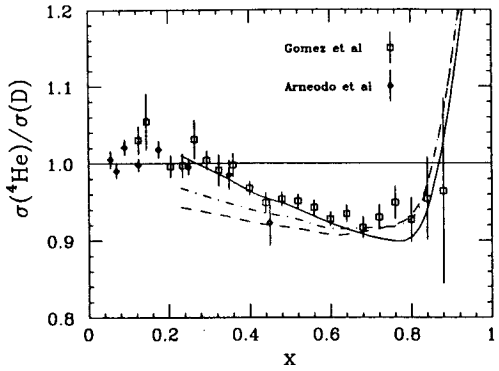

Figure 9: Results for the ^{4}He to deuterium cross section ratios, compared to the experimental data of [30, 37]. The solid line gives the full result including the pion contribution, the dashed-dot and dashed lines give the result obtained using the deForest prescription with and without excess pion contributions (see below).

spectral function appears to be erroneous. Also note that the value $\langle\delta\nu\rangle =$ 98,eV obtained from the realistic spectral function is not far from the lower bound.

In fig.9 we show our results for ^{4}He, and compare them to the available data for this nucleus.

From figs.8 and 9 we conclude that our approach explains the ratio at large x, in the region where this ratio has the pronounced dip. All previously explored approaches, except the ones like the rescaling models which have a free parameter to fit the data, always produced too small an effect in this region.

6 Relation to other approaches

In a number of papers [15, 16], Q^2-rescaling has been advocated as a means to explain the EMC-effect. This rescaling idea is quite successful, although the physical basis of the recipe is not so clear. In our description of deep inelastic scattering, we naturally find some "rescaling" in terms of *both* x and Q^2.

We have numerically studied the effect of the rescaling inherent to our

treatment of deep inelastic scattering. The results obtained using the deForest prescription are shown in fig.10. The solid curve shows again the full result obtained using eq.(30) valid in the Bjorken limit, which is very close to the one obtained from eq.(22). The dashed curve corresponds to eq.(30) but with $\tilde{Q}$ replaced by Q. In the present approach the Q^2 rescaling factor of $\sim$1.25 is quite small compared to the factor close to 2 as in [16] and results from a physical model for the scattering process rather than an *ad hoc* recipe.

In fig.10 we also show the result obtained using eq.(30) with $\tilde{Q}$ replaced by Q and omitting the factor $1/(1+\delta\nu/mx)$. This corresponds to the standard convolution formula, but with $\tilde{x}$ rather than x'. The $(1+\delta\nu/mx)$ factor in the denominator is primarily responsible for making the EMC ratio smaller than one. As mentioned earlier, this factor basically comes from using $\tilde{k}, \tilde{q}$ in eq.(11) as required in the PWIA treatment of nuclear binding.

The dotted curve in fig.10 gives the ratio predicted by the standard convolution eq.(31). The difference between that and the dash-dot curve is due to that between $\tilde{x}$ and x'.

An alternative to the standard convolution model has been also explored in ref.[18] where the authors take into account the off-shellness of the struck particle using a relativistic formalism. This approach, as ours, tries to deal

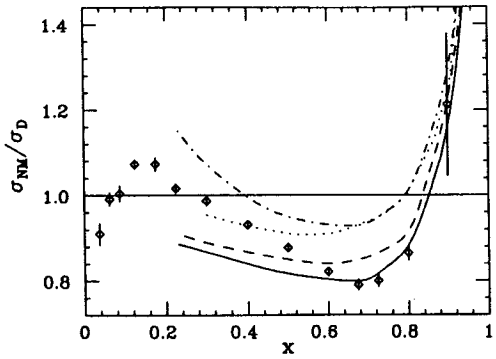

Figure 10: The solid curve gives our full result, the dashed curve gives the result of eq.(30) with $\tilde{Q}$ replaced by Q. The dotted curve corresponds to the standard convolution approximation, eq.(31). The dashdot curve corresponds to eq.(30), with $\tilde{Q}$ replaced by Q and the factor $1/(1+\delta\nu/mx)$ omitted.

with deep inelastic scattering from an off-shell nucleon by providing a physical model that lets one ultimately use the measured on-shell structure functions of the nucleon. The resulting alternative convolution formula then involves the free space structure function $F_2^N(Q^2,x)$ evaluated at a shifted value of the argument. The approach of ref.[18] provides a fairly good description of the measured EMC ratios at $x > 0.5$, while the data at lower x are sizably underestimated.

7 Contribution of pions

The comparison between our calculated results, shown in figs.8 and 9, and the data shows that our calculation does not reproduce the data at the lower values of x. This is to be expected. For very low x ($x < 0.1$) the cross section ratios exhibit the shadowing effects which are well explained in terms of the vector dominance model [41] which contains additional physics not addressed in the present paper. This region is thus outside of the scope of the present work. For larger x-values the contribution of virtual pions, present as a consequence of the pion-exchange nature of the nucleon-nucleon force, is important. This pionic contribution is closely related to nuclear binding, and will be briefly considered below.

We have not yet calculated the pionic contribution in a manner entirely

consistent with the nucleonic contribution as discussed above. That will require knowledge of the removal spectral function of pions in nuclear matter, which is not yet available. In order to gauge the effect of the pionic contribution on the EMC ratio, we will simply add to our calculated nucleonic EMC-effect the effect of pions as calculated by Berger *et al.*[42].

Berger *et al.* use the parton model to compute the nucleon structure functions, from quark and antiquark densities determined by experiment [43]. For the pion they also use the (rather poorly known) experimental structure function [44]; the results are quite insensitive, however, to the pion structure function used. The pionic effect computed refers exclusively to the *excess* pions associated with nuclear binding, and not the pionic densities associated with the pion cloud of the isolated nucleon.

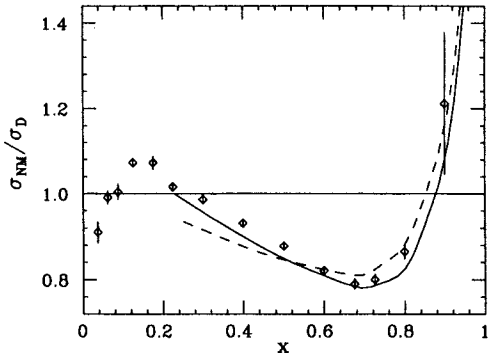

Figure 11: The full curve gives our result, supplemented by the contribution of the pions as calculated by Berger *et al.*, scaled to the number of pions in nuclear matter as calculated by Friman *et al.*. The dashed curve gives the same result, but by using the deForest prescription.

The number of excess pions in nuclear matter and light nuclei has been calculated in the static approximation by Friman *et al.*[45] starting from the Argonne v_{28} model for the nucleon-nucleon force. The ratio of excess pions to nucleons in nuclear matter, ^{4}He, ^{3}He and deuteron is predicted to be 0.18, 0.09, 0.05 and 0.024, respectively. The results of Berger *et al.* for deep inelastic scattering from excess pions were computed for a ratio of 0.22. We scale them with the predicted values of the ratio to estimate the excess pion contribution to deep inelastic scattering cross section. As can be seen from figs.9,11, inclusion of the pionic contribution of Berger *et al.*

clearly improves the agreement with the data, although, depending on the treatment of $\widetilde{W}_{\mu\nu}$, a small difference remains. We estimate that the difference between the two curves shown in fig.11 represents the theoretical uncertainty in the treatment of current conservation. We intend to calculate the pionic contribution with an approach consistent with the one employed here for the nucleonic contribution in the future.

8 Results for ^{3}He

Even though there are no data available for the EMC ratio of ^{3}He, this nucleus is often used as a polarized neutron target to study spin dependent structure functions. We present here our predictions for the EMC ratio, to provide an estimate of nuclear binding effects on deep inelastic scattering from ^{3}He.

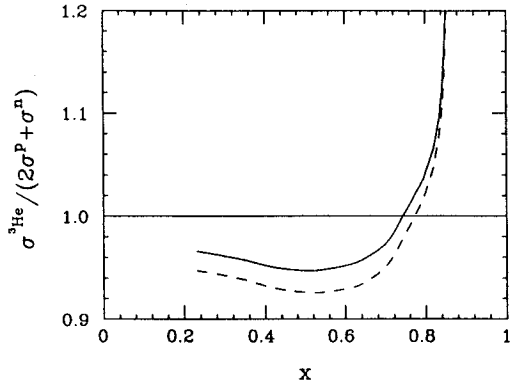

Figure 12: The full curve gives our result for ^{3}He calculated using the spectral function for the Paris potential, the dashed line gives the result for the Argonne v14+Urbana VII interaction.

Fig.12 shows the ratios

$$R_{^3He} = \frac{d^2\sigma_{^3He}}{(2d^2\sigma_p + d^2\sigma_n)} , \qquad (42)$$

obtained from spectral functions calculated by the Hannover group [46] with the Paris potential [47] and from variational wave functions obtained from Argonne v_{14} + Urbana VII interactions [8]. As can be seen, $R_{^3He}$ has a rather

weak model dependence, the difference between the solid and dashed curve of Fig.12 being always less than 2.5% over the whole range of x. The more pronounced dip exhibited by the dashed line, corresponding to the Argonne v_{14} potential, reflects the presence of stronger high momentum components in the ^{3}He wave function, leading to an expectation value of the potential energy $< v_{ij} >= -53.9$ MeV [48], to be compared to the Paris potential result $< v_{ij} >= -50.4$ MeV [49]. Both curves in fig.12 include the excess pion contribution.

9 Conclusions

In this paper, we have studied the EMC effect in the region of the Bjorken scaling variable $x > 0.1$. We have investigated in detail the influence of the binding of nucleons in nuclei, without considering any of the more "exotic" effects discussed in the literature [1, 2]. As compared to the many previous theoretical studies of the EMC effect we have improved the treatment of nuclear binding in two respects:

1. We have studied the EMC effect in *infinite nuclear matter* and ^{4}He rather than the medium-A nuclei usually considered. For both infinite nuclear matter and ^{4}He theoretical calculations of the wave function of high quality can be performed, both for the long- and the short-range aspects of the wave function. For a process of large momentum transfer — such as deep inelastic scattering – the spatial resolution is very good. A reliable treatment of the short-range properties of the wave function resulting from two-nucleon correlations then is very important.

2. We have treated explicitly the off-shell nature of the nucleon on which the DIS process occurs. This is necessary to achieve a well defined relation between off- and on-shell DIS structure function of the nucleon, as only the latter one is known experimentally.

The calculated values of the EMC ratios have been compared to the data for helium and infinite nuclear matter. The latter have been determined from the world-supply of data for finite nuclei, and the resulting nuclear matter to deuteron-ratios thus incorporate *all* data on nucleus to deuteron-ratios measured.

We find that a good theoretical description of nuclear binding including the short-range properties is very important. Nuclear binding allows to quantitatively understand the cross section ratios at the larger x where the biggest deviation of the cross section ratio from one occurs. At these larger x, no effect beyond binding, and no model assumption involving free parameters, are needed to understand the EMC ratios.

At the smaller values of x, the calculated ratios again agree well with the data provided the contribution of excess pions, also related to nuclear

binding, is taken into account. For an entirely consistent prediction of the contribution of the excess pions, the pion removal spectral function will have to be calculated.

Overall, the agreement between our parameter-free calculation and the data is very good. From this agreement we conclude that the consequences of nucleon binding explain the bulk of the EMC effect for $x > 0.1$; no "exotic" effects seem to be needed.

References

[1] M. Arneodo, *Phys. Rep.* 240 (1994) 301.

[2] D.F. Geesaman, K. Saito, and A.W. Thomas, *Ann. Rev. Nucl. Part. Sci.* 45 (1995) 337.

[3] T.N. Taddeucci et al, *Phys. Rev. Lett.* 73 (1994) 3516.

[4] O. Benhar, A.Fabrocini, S. Fantoni, G.A. Miller, V.R. Pandharipande, and I. Sick, *Phys. Rev.* C44 (1991) 2328.

[5] O. Benhar, A. Fabrocini, S.Fantoni, V.R. Pandharipande, and I. Sick, *Phys.Rev.Lett.* 69 (1992) 881.

[6] O. Benhar, A. Fabrocini, S. Fantoni, and I. Sick, *Phys. Lett* B343 (1995) 47.

[7] O. Benhar, A. Fabrocini, S. Fantoni, and I. Sick, *Phys. Lett. B* 343 (1995) 47.

[8] O. Benhar and V.R. Pandharipande, *Phys.Rev.* C47 (1993) 2218.

[9] T. de Forest, *Nucl. Phys.* 392 (1983) 232.

[10] O. Benhar, V.R. Pandharipande, and I. Sick, *Phys. Lett. B* 410 (1997) 79.

[11] C. Itzykson and J.B. Zuber, *Quantum Field Theory. McGraw-Hill, New York*, 1980.

[12] A.Amroun, V. Breton, J.-M. Cavedon, B. Frois, D. Goutte, J. Martino, X.-H, Phan, S.K. Platchkov, I. Sick, and S. Williamson, *Phys.Rev.Lett.* 69 (1992) 253.

[13] W.B. Atwood and G.B. West, *Phys. Rev. D* 7 (1973) 773.

[14] A.E.L. Dieperink, T. de Forest, I. Sick, and R.A. Brandenburg, *Phys. Lett.* 63B (1976) 261.

[15] O. Nachtmann and H.J. Pirner, *Z. Phys.* C21 (1984) 277.

[16] F.E. Close, R.G. Roberts, and G.G. Ross, *Phys. Lett.* 129B (1983) 346.

[17] C. Ciofi degli Atti and S. Liuti, *Phys. Lett.* B225 (1989) 215.

[18] F. Gross and S. Liuti, *Phys.Rev. C* 45 (1992) 1374.

[19] O. Benhar, A. Fabrocini, and S. Fantoni, *Nucl. Phys.* A505 (1989) 267.

[20] D.S. Koltun, *Phys. Rev.* C9 (1974) 484.

[21] D. Day, J.S. McCarthy, Z.E. Meziani, R. Minehart, R.M. Sealock, S. Thornton, J. Jourdan, I. Sick, B.W. Filippone, R.D. McKeown, R.G. Milner, D. Potterveld, and Z. Szalata, *Phys.Rev.C* 40 (1989) 1011.

[22] D. Day I. Sick, *Phys.Lett.* B274 (1992) 16.

[23] A. Bodek, N. Giokaris, W.B. Atwood, D.H. Coward, D.J. Sherden, D.L. Dubin, J.E, Elias, J.I. Friedman, H.W. Kendall, J.S. Poucher, and E.M. Riordan, *Phys. Rev. Lett.* 50 (1983) 1431.

[24] S. Stein, W.B. Atwood, E.D. Bloom, R.L.A. Cottrell, H. DeStaebler, C.L. Jordan, h.G.Piel, C.Y. Prescott, R. Siemann, and R.E. Taylor, *Phys. Rev. D* 12 (1975) 1884.

[25] G. Bari *et al. Phys. Lett.* 163B (1985) 282.

[26] A.C. Benvenuti *et al, Phys. Lett.* 195B (1987) 91.

[27] J. Ashman et al, *Phys. Lett.* 206B (1988) 364.

[28] J. Ashman *et al. Z. Phys. C* 57 (1993) 211.

[29] J. Ashman*et al. Phys.Lett* B202 (1988) 603.

[30] J. Gomez *et al. Phys. Rev. D* 49 (1994) 4348.

[31] P. Amaudruz *et al, Z.Phys.C* 51 (1991) 387.

[32] P. Amaudruz *et al, Z.Phys.C* 53 (1992) 73.

[33] M. Arneodo *et al. Nucl. Phys. B* 441 (1995) 12.

[34] J. Aubert *et al. Phys. Lett.* 123B (1983) 275.

[35] S. Dasu *et al. Phys. Rev. D* 49 (1994) 5641.

[36] O. Benhar, V.R. Pandharipande, and I. Sick, *in preparation.*

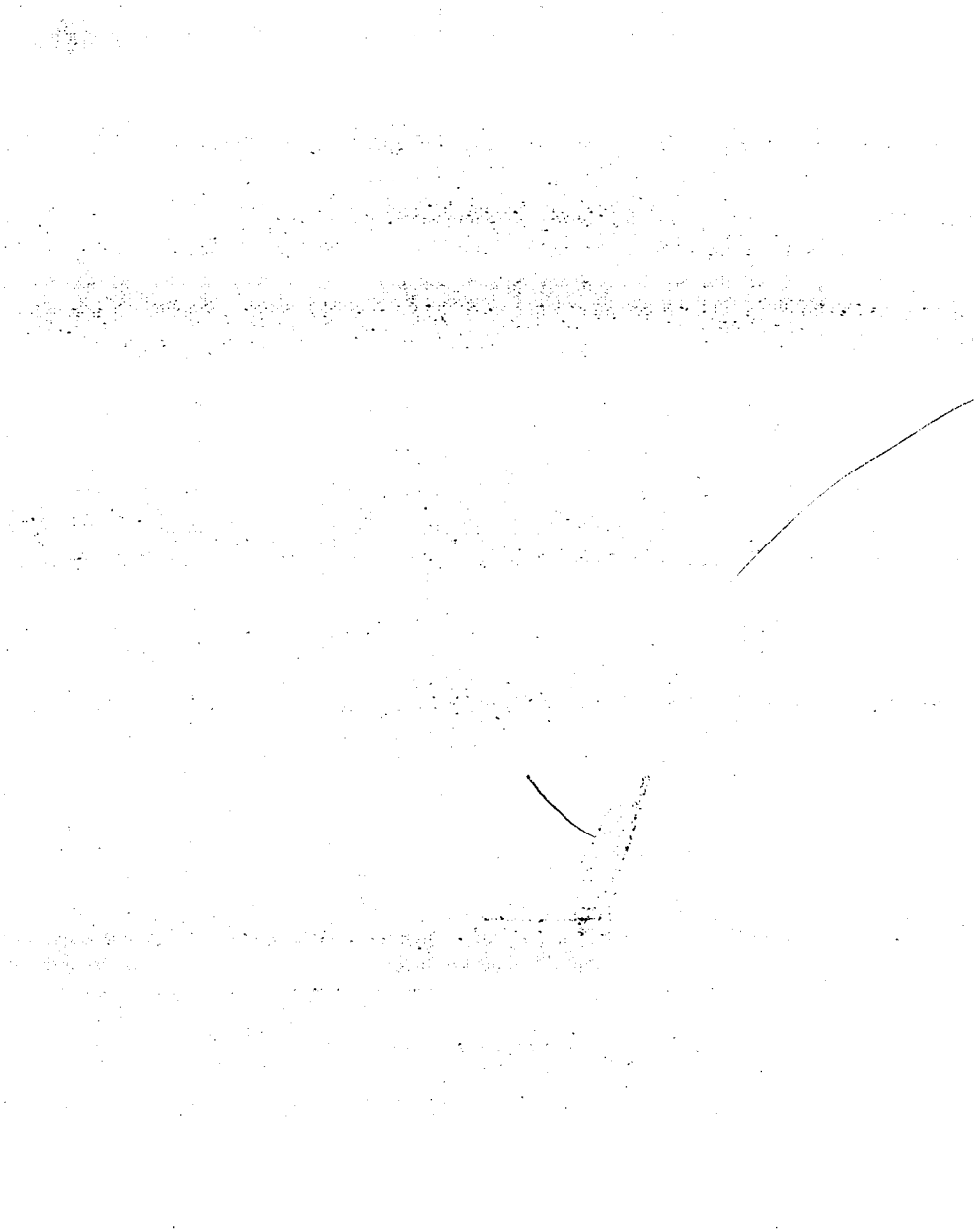

[37] P. Arnaudruz *et al. Nucl. Phys. B* 441 (1995) 5.

[38] S. Rock, R.G. Arnold, P.E. Bosted, B.T. Chertok, B.A. Mecking, I. Schmidt, Z.M, Szalata, R.C. York, and R. Zdarko, *Phys. Rev. D* 46 (1992) 24.

[39] I.E. Lagaris and V.R. Pandharipande, *Nucl. Phys.* A359 (1981) 331.

[40] A. Bodek, M. Breidenbach, D.L.Dubin, J.E. Elias, J.I. Friedman, H.W.Kendall, J.S.Poucher, E.M. Riordan, M.R. Sogard, D.H. Coward, and D.J. Sherden, *Phys. Rev.* D20 (1979) 1471.

[41] G. Piller, W. Ratzka, and W. Weise, *Z. Phys.* A352 (1995) 427.

[42] E.L. Berger, F.Coester, and R.B. Wiringa, *Phys. Rev. D* 29 (1984) 398.

[43] H.Abramowicz et al, *Z. Phys.* C25 (1984) 29.

[44] J. Badier et al, *Z. Phys.* C18 (1983) 281.

[45] B.L. Friman, V.R. Pandharipande, and R.B. Wiringa, *Phys. Rev. Lett.* 51 (1983) 763.

[46] H. Meier-Hajduk, C. Hajduk, P.U. Sauer, and W. Theis, *Nucl. Phys.* A395 (1983) 332.

[47] M. Lacombe *et al, Phys. Rev. C* 21 (1980) 861.

[48] R. Schiavilla, V.R. Pandharipande, and R.B. Wiringa, *Nucl.Phys.* A449 (1986) 219.

[49] C. Hajduk and P.U. Sauer, *Nucl. Phys. A* 369 (1981) 321.